Intelligent Diagnosis of Open and Short Circuit Faults in Electric Drive Inverters For Real-Time Applications

M. Abul Masrur*, Senior Member, IEEE, ZhiHang Chen**, and Yi Lu Murphey**, Senior Member, IEEE

* US Army RDECOM-TARDEC, Warren, MI 48397, USA (email: md.abul.masrur@us.army.mil).
**Univ. of Michigan-Dearborn, Dearborn, MI 48128, USA (email: yilu@umich.edu).

***Abstract* — This paper presents a machine learning technique for fault diagnostics in induction motor drives. A normal model and an extensive range of faulted models for the inverter-motor combination were developed and implemented using a generic commercial simulation tool to generate voltages and current signals at a broad range of operating points selected by a machine learning algorithm. A structured neural network system has been designed, developed and trained to detect and isolate the most common types of faults: single switch open circuit faults, post-short circuits, short circuits, and the unknown faults. Extensive simulation experiments were conducted to test the system with added noise, and the results show that the structured neural network system which was trained by using the proposed machine learning approach gives high accuracy in detecting whether a faulty condition has occurred, thus isolating and pin-pointing to the type of faulty conditions occurring in power electronics inverter based electrical drives. Finally, the authors show that the proposed structured neural network system has the capability of real-time detection of any of the faulty conditions mentioned above within 20 milliseconds or less.**

***Index Terms* — fault diagnostics, open circuit fault, short circuit fault, model-based diagnostics, machine learning, power electronics, inverter, motor, electric drives, neural networks, electric vehicle, hybrid vehicle, field oriented control.**

1 INTRODUCTION

A large number of industrial drives, including some used in electric vehicles (EV) and hybrid electric vehicles (HEV) [1], consist of three-phase induction motor drives and associated power electronics based inverter, together with the necessary control system [1]. The precise torque control of these motors has been made possible by power electronics with controllable solid state switches and the Field Oriented Control (FOC) techniques [2-5]. However, the solid state switches can fail by being "open" or "shorted", and the reverse diodes in the switches can also fail. This paper presents an intelligent system approach to the problem of real time detection of the open, short, and post short-circuit faults in inverter switches.

There exists a good amount of work in the literature [6-7] on fault diagnostics of internal combustion (IC) engine vehicles. However, for electric or hybrid vehicles, fault diagnostic techniques have not been well investigated yet, since EV/HEV is still in the relatively early stage in the automotive industry compared to IC engine vehicles. A closely related work by Ribeiro, Jacobina and Silva [8], was based on the direct comparison of voltages measured at a few key points of the system with application to an electric drive in which the effect of closed loop control is not considered. Additional references exist in the area of diagnostics in the motor and power inverters [9-14]. There are a number of intelligent systems approaches which have been investigated in signal fault diagnosis. Rule-based expert systems and decision trees are two traditional diagnostic techniques, but they have serious limitations. A rule-based system often has difficulties in dealing with novel faults and acquiring complete knowledge to build a reliable rule-base. A decision tree can be very large for a complex system, and it is

Report Documentation Page

Form Approved
OMB No. 0704-0188

1. REPORT DATE	2. REPORT TYPE	3. DATES COVERED
03 MAR 2009	**N/A**	**-**

4. TITLE AND SUBTITLE	5a. CONTRACT NUMBER
Intelligent Diagnosis of Open and Short Circuit Faults in Electric Drive Inverters For Real-Time Applications (PREPRINT)	5b. GRANT NUMBER
	5c. PROGRAM ELEMENT NUMBER
6. AUTHOR(S)	5d. PROJECT NUMBER
M. Abul Masrur; ZhiHang Chen; Yi Lu Murphey	5e. TASK NUMBER
	5f. WORK UNIT NUMBER
7. PERFORMING ORGANIZATION NAME(S) AND ADDRESS(ES)	8. PERFORMING ORGANIZATION REPORT NUMBER
US Army RDECOM-TARDEC 6501 E 11 Mile Rd Warren, MI 48397-5000, USA Univ. of Michigan-Dearborn, Dearborn, MI 48128, USA	**19740RC**
9. SPONSORING/MONITORING AGENCY NAME(S) AND ADDRESS(ES)	10. SPONSOR/MONITOR'S ACRONYM(S)
	TACOM/TARDEC
	11. SPONSOR/MONITOR'S REPORT NUMBER(S)
	19740RC

12. DISTRIBUTION/AVAILABILITY STATEMENT
Approved for public release, distribution unlimited

13. SUPPLEMENTARY NOTES
Submitted for publication in IET-Power Electronics (Journal), The original document contains color images.

14. ABSTRACT

15. SUBJECT TERMS

16. SECURITY CLASSIFICATION OF:			17. LIMITATION OF ABSTRACT	18. NUMBER OF PAGES	19a. NAME OF RESPONSIBLE PERSON
a. REPORT	b. ABSTRACT	c. THIS PAGE			
unclassified	**unclassified**	**unclassified**	**SAR**	**20**	

also system dependent such that even small engineering changes can mean significant updates [14]. More recently model based approaches, fuzzy logic, artificial neural networks (ANN), case based reasoning (CBR) are popular techniques used in various fault diagnostics problems in electrical systems. In particular ANN's have been shown to be effective in many automotive fault diagnostic applications [15-18]. In this research the authors apply the neural network technology for detecting and locating multi-classes of faults in the electric drive inverters.

In this paper the authors present the state of the art diagnostic technologies based on machine learning, and a model that simulates a closed loop field oriented control based electric drive to generate multiple quantitative attributes of various signals including the torque, and voltages and currents in all phases. Specifically, this research attempts to solve the following problem with reference to Fig. 1: *"For a six-switch inverter driven three-phase induction motor under closed-loop control, given two current sensors in the output inverter lines (which is same as the motor line connections), and two voltage sensors across the lines, an intelligent diagnostic system should be developed to identify in real time whether there are any faulty inverter switches, assuming that only one of the six switches, or two switches on the same limb, can fail at a given time, and that the faulty condition can be either an open, a short, or a post-short type".* The term "post-short circuit" has been defined in detail in section 2. A limited amount of literature on inverter fault diagnostics is available [5, 8] where the effect of closed loop control is not included, and no other literature to the knowledge of the authors has reported on fault diagnostics in closed loop situations. Furthermore, this research extends far beyond the detection of fault occurrences in a closed loop electric system. This paper presents a structured neural network system that is trained to detect and locate (isolate), in real time, 15 different faulty conditions in either open or closed loop situations, and detect unknown faults.

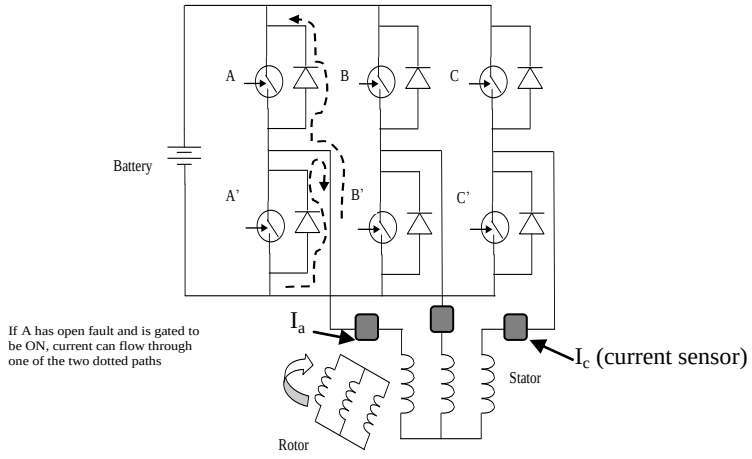

Figure 1. A six-switch inverter in a three-phase electric drive model.

This work builds upon, but extends significantly beyond the authors' previous work on intelligent diagnostics in electric drives [19-21]. In [19], the authors proposed a machine learning algorithm that automatically generates training data at critical

operation points in a six-switch inverter and showed that this machine learning approach is effective when it was used to train a robust diagnostic system for detecting single switch broken faults. In [20-21] the authors presented a model based approach for fault diagnosis in electric drives under both open- and closed-loop controls. The model was for a six-switch inverter driven three-phase induction motor, implemented by using a generic commercial simulation tool [22] to generate the normal operating signals and the faulty signals. The model was used to generate two types of faults: single switch faults and post-short circuit faults. An innovative machine learning framework was presented that involves an algorithm that automatically selects a set of representative operating points in the torque-speed domain, and the training of a diagnostic neural network for the detection of single switch faults and post short circuit faults. The authors showed excellent results on the data generated by a simulation program and an experimental bench setup [20]. In order to make this paper reasonably self-contained within the limited amount of space, the authors have included the necessary information from their previous work wherever appropriate. More information regarding the authors' related work can be found in reference [20].

In this paper, the authors extend the six-switch inverter driven three-phase induction motor model to include the short circuit faults. There can be 15 classes of faults occurring in the six-switch inverter, namely: 6 single switch open circuit faults, 3 post-short-circuit conditions, and 6 short circuit faults. The authors present a real-time fault detection system that has the capabilities of robustly detecting and accurately locating these faults immediately after they occur. The real-time fault detection system is developed using a structured neural network. The authors will show that the diagnostic system has the capability of accurately detecting whether a fault has occurred, whether it is open circuit, short circuit, or post short-circuit fault, and pin-pointing to the faulty location in the electric drive within 20 milliseconds or less. The contribution of this paper is important because in many applications it is extremely important to detect a fault immediately after it occurs and pin-point to the cause of fault. As soon as a fault is detected and located, e.g. switch A short or C’ open etc., it should be isolated and the damaged part should be shut down immediately to minimize the damage to other parts of the system. Identifying the location and type of the fault fast enough can also allow smooth transition to a gracefully degradable mode, which enhances the overall system availability.

The authors also want to point out the challenges involved in generating short circuit faults, which constitute the additional type of faults presented in this paper. In this paper the short circuit fault condition in the induction motor is simulated in a closed-loop control environment. In a physical setting, an induced short circuit fault can cause significant damage (if not total destruction) to the closed-loop controlled electrical system. To prevent such a situation, an electrical system in a lab setting needs various protective mechanisms built in it to shut down the system before any signals in a faulty condition can be sampled. Regarding the possibility of setting up hardware based experiment where catastrophic failure will not occur during a short

circuit fault, it should be noted that this catastrophic failure pertains initially to the solid state power electronic switches, which will try to short circuit the source. Hence, to save the system (both the source and the power electronics switch) one has to trip it off. Otherwise the source itself, in addition to the switch, may suffer damage. The issue, therefore, is more related to be able to diagnose the fault before it is tripped off. Otherwise the power electronics circuit can soon become unbalanced. At that point, if the motor still has mechanical load connected to it, the situation can lead to both electrical and mechanical damage to the motor due to unbalanced operation. The authors noted earlier in this paper about the possibility of degradable mode of operation. It is possible to operate in such a mode while the system is unbalanced (within some limitations). However, that needs the initiation of an alternate control path in the motor control algorithm, which is not within the scope of this paper. Unless the motor control algorithm is altered properly during unbalanced condition, the motor drive system can undergo damage (both mechanical and electrical). All the above items point to the difficulty of designing a physical experiment under the above circumstances. Therefore, the authors believe that simulated systems are important means to study fault diagnostic problems in closed-loop situation. Due to these difficulties, the results generated in the paper are primarily from the data produced by a simulation model. The simulation model has been validated on the single open switch faults and post-short circuit faults by a lab bench setup [20]. In order to enrich the studies using simulation for short circuit faults, the authors present in this paper the fault detection results on signals generated with different degrees of noise.

This paper is organized as follows. Section 2 presents the closed-loop electric drive model that has the capability of simulating a broad range of faults: single open switch, post-short, and short circuit faults. Section 3 presents a multi-class neural network framework for the diagnosis of 15 classes of faulty conditions in an electric drive. Section 4 presents the real-time fault detection neural network system. Section 5 gives the summary and conclusion.

2 MODELING OF THE ELECTRIC DRIVE SYSTEM FOR FAULT-DIAGNOSTICS

In [20-21] the authors developed a simulation model of a closed loop electric drive system in an EV or HEV that simulates single switch open and post short circuit faults. This section gives a quick review of this model and describes the extension of the model to simulate short circuit faults.

In this model electromechanical torque is the feedback quantity to the controller, which compares it against a reference signal, and takes control actions accordingly. The controller is an indirect FOC [2-3] that generates a reference three-phase voltage signal. The reference voltage signal is then fed to the inverter pulse width modulation (PWM) algorithm to initiate voltage generation [2-3]. The job of the controller ends with the generation of gating signals to the inverter switches, and the situation thereafter is depicted in Figure 1. Since the scope of this paper is on fault diagnostics and not the already well known

FOC techniques for motor control, the authors will not delve into the details of modeling, simulation, and control, and go through those very briefly in this section, since the references indicated earlier contain abundant details on those. The motor electro-mechanical system is described by the following standard set of differential and algebraic equations with d-q axis fixed in the stator [1-3], where R_s and R_r are the stator and rotor resistances, L_s and L_r are the stator and rotor self inductances, M is the stator/rotor mutual inductance, ω_r is the electrical rotor angular velocity, V_{ds} and V_{qs} are the d and q axis stator voltages, I_{ds} and I_{qs} are the d and q axis stator currents, I_{dr} and I_{qr} are the d and q axis rotor currents, and p is the differential operator d/dt. The rotor is assumed to be shorted and hence the voltages are 0 in equation (1).

$$\begin{bmatrix} V_{ds} \\ V_{qs} \\ 0 \\ 0 \end{bmatrix} = \begin{bmatrix} (R_s + pL_s) & 0 & pM & 0 \\ 0 & (R_s + pL_s) & 0 & pM \\ pM & \omega_r M & (R_r + pL_r) & \omega_r L_r \\ -\omega_r M & pM & \omega_r L_r & (R_r + pL_r) \end{bmatrix} \begin{bmatrix} I_{ds} \\ I_{qs} \\ I_{dr} \\ I_{qr} \end{bmatrix} \quad (1)$$

The electromagnetic torque is given by $T_e = (3/2)\,(P/2)\,M\,\{I_{qs}\,I_{dr} - I_{ds}\,I_{qr}\}$, where P is the number of poles. The mechanical equation of motion for the motor shaft is given by $T_e - T_L = J\,(d\omega_m/dt) + B\omega_m$, where ω_m is the mechanical shaft speed, T_L is the load torque, J is the moment of inertia, and B is the friction coefficient. The authors have fully implemented this model by using generic commercial software [20-22], and for convenience the implemented model will be referred as "SIM_drive" in this paper.

The various states of the switches and the corresponding voltages applied to the motor are indicated in Table I for normal condition, and in Tables II and III for one switch open and short circuit conditions respectively. In these tables, the symbol V_{An} (or V_{Bn}, or V_{Cn}) means voltage between line "A" (or "B", or "C") and the neutral point "n" of the Y-connected stator winding of the induction motor, and E is the battery voltage. The authors used this model to simulate 15 different faulty conditions, namely, 6 classes of single switch open, 3 classes of post-short circuits, and 6 classes of short circuits.

Table I: Switching table for normal operation of the switch

STATE #	SWITCH A	SWITCH B	SWITCH C	V_{AN}/ E	V_{BN}/ E	V_{CN}/ E
Null	0	0	0	0	0	0
1	0	1	0	-1/3	2/3	-1/3
2	0	1	1	-2/3	1/3	1/3
3	0	0	1	-1/3	-1/3	2/3
4	1	0	1	1/3	-2/3	1/3
5	1	0	0	2/3	-1/3	-1/3
6	1	1	0	1/3	1/3	-2/3
Null	1	1	1	0	0	0

Table II: Switching table for faulted operation in which switch A is permanently open. [23]

STATE #	SWITCH A	SWITCH B	SWITCH C	V_{AN} / E	V_{BN} / E	V_{CN} / E
Null	0	0	0	0	0	0
1	0	1	0	-1/3	2/3	-1/3
2	0	1	1	-2/3	1/3	1/3
3	0	0	1	-1/3	-1/3	2/3
4	0	0	1	-1/3 or 1/3	-1/3 or -2/3	2/3 or 1/3
5	0	0	0	0 or 2/3	0 or -1/3	0 or -1/3
6	0	1	0	-1/3 or 1/3	2/3 or 1/3	-1/3 or -2/3
Null	0	1	1	-2/3 or 0	1/3 or 0	1/3 or 0

Table III: Switching table for shorted operation in which Switch A is permanently shorted

STATE #	SWITCH A	SWITCH B	SWITCH C	V_{AN}/ E	V_{BN}/ E	V_{CN}/ E
Null	1	0	0	0	0	0
1	1	1	0	0	0	0
2	1	1	1	0	0	0
3	1	0	1	0	0	0
4	1	0	1	1/3	-2/3	1/3
5	1	0	0	2/3	-1/3	-1/3
6	1	1	0	1/3	1/3	-2/3
Null	1	1	1	0	0	0

In the "post short-circuit" condition, a complete burn out of a switch pair can happen (with both the upper and lower switches in a particular limb open due to burn out, which can take place if the upper switch is stuck-short and shortly thereafter the lower switch is gated to be ON), due to a power supply short circuit through the switches which is not cleared. Under this condition (with both switches in a limb burned out), in order to perform the simulation the dynamic equations of the three phase machine have to be restructured, with the phase current corresponding to the burned out switch pair set to zero. It should be noted that when a particular phase current of the machine remains totally zero all the time, it is not possible to create a table in the same manner as Table II, due to the fact that the particular limb is open with infinite impedance. With reference to Table II (state # 4 to 7), under open fault condition the current can flow through one of the two possible paths (e.g. the dotted lines in Figure 1) based on the current that was flowing in the motor windings at the moment of the occurrence of the fault. Hence, in this case there are two possible voltage values that can be imposed on the line to neutral of the motor windings, depending on which current path is used. For example, if the current is flowing through the upper diode, then corresponding to state # 4 one needs to select the status of switches A=1, B=0, C=1, and conversely it will be A=0, B=0, C=1 if the current was flowing through bottom diode. Consider the former case, which implies $V_{An} = V_{Cn}$, and $V_{An} - V_{Bn} = E$, the battery voltage. These two equations by themselves are not sufficient to give the phase voltage values to be used in equations in (1) for all the three phases. The other condition, which is not an assumption, and is based on the stator and rotor circuit flux linkages using circuit theory, is that the summation of three line to neutral voltages for the phases in the motor is equal to zero or $V_{An} + V_{Bn} + V_{Cn} = 0$. This condition is valid provided the three currents in the stator and rotor circuit in the induction motor adds up to zero (which is true in a 3 phase induction motor without a return neutral line, and is due to the winding topology), and provided that the individual phases A, B, and C has identical (or symmetrical) windings for both the stator and the rotor. Sometimes there is a misconception

that this relationship between the phase voltages with the input dc voltage (based on Table II) is only valid during a steady state balanced operation, but in reality it is valid under unbalanced operations as well (like open fault) indicated earlier, subject to the restrictions given above [23]. Once this last condition is in place, it results in V_{An} = 1/3 E, V_{Bn} = -2/3 E, V_{Cn} = 1/3 E. Similar derivations apply to other switching states.

Table IV shows the operating conditions used in the simulation of these models.

Table IV: The operating conditions used in the sine-PWM-closed-loop model

VARIABLE NAME	DESCRIPTION	VALUE
V_{DC}	DC voltage provided by battery	500V
PWM carrier Frequency	Frequency of the sine wave	8 kHz
Speed	Synchronous speed of the motor	60, 300, 600, 900, 1800 rpm
Reference torque command	Mechanical torque desired from the motor	10, 50, 100, 200 Nm
Simulation time	Simulation Time	6.25s
Trigger Time	Time point to trigger the fault condition	0.25s
Sampling rate	Sampling rate to get the output data.	0.001s
Number of data points	Number of data points	6000

Examples of the various voltage, current, and torque profiles under different fault conditions are shown in Figs. 2(a), 2(b) and 2(c), and 2 (d). Note, the authors show only the data points in the first 100 ms in all the graphs in Fig. 2. Since the values can go very high in these situations, it is difficult to depict all the curves within a readable range in a single diagram. The intention of the plots, however, is to show the overall qualitative view, rather than finer numerical details (which are handled by the algorithm during sampling, training, and diagnostic processes). It should be noted, as the figures indicate, that under certain fault conditions the current and torque can very quickly well exceed the rated limits of the machine and power electronic switches. In a real system, however, the machine will need to be disconnected (or reconfigured) before it exceeds the limits, in order to protect the system. However, the authors' methodology allows the detection of the fault within a very short time after its inception. It is the future plan of the authors to further extend this work to include appropriate protection and/or reconfiguration mechanisms after such faults.

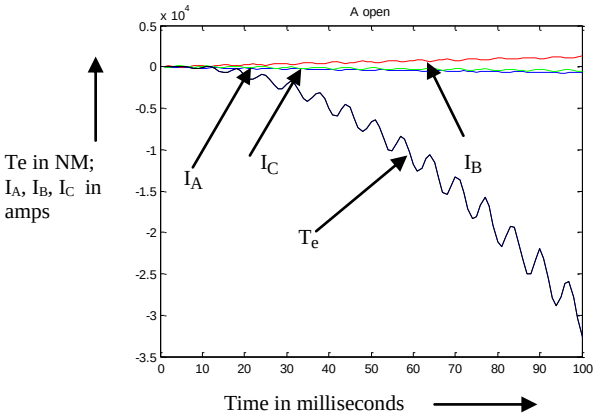

(a). Signals I_A (in blue), I_B (in red), I_C (in green) and Te (in black) when switch A is open

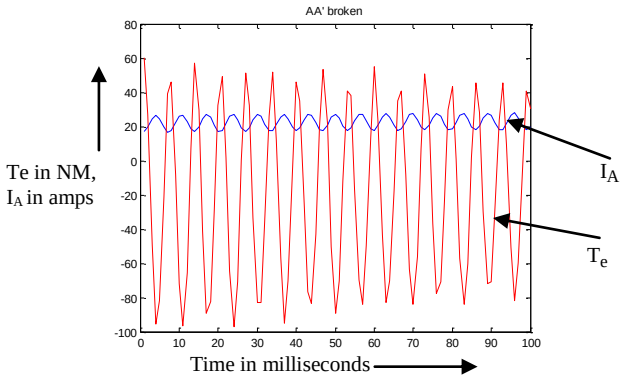

b). Signals I_A (in blue) and T_e (in red) when switches AA' are broken

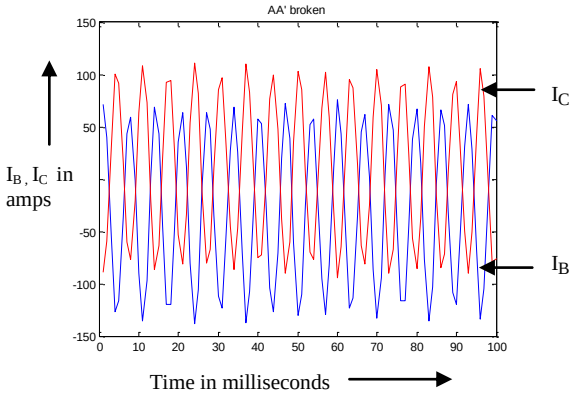

(c). Signals I_B (in blue) and I_C (in red) when Switches AA' are broken.

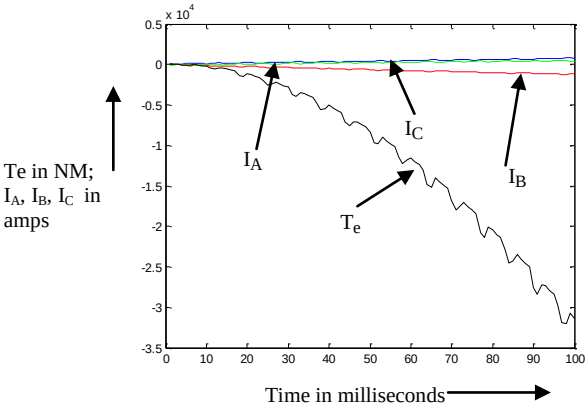

(d). Signals I_A (in blue), I_B (in red), I_C (in green) and Te (in black) when Switch A is shorted.

Figure 2. Plots showing currents, I_A, I_B, I_C, and Torque Te under various fault conditions at operating point: torque=100 nm, speed=600 rpm. Time is in msec.

3 ELECTRICAL DRIVE FAULT DETECTION USING SIGNAL ANALYSIS AND ARTIFICIAL NEURAL NETWORKS

The authors developed a multi-class neural network framework for the detection and isolation of a broad range of faulty conditions in an electrical drive. A multi-class neural network system requires the careful design of its input and output spaces, neural network architecture, selection of training parameters and training data [24-33]. In this application, the authors define the input space as a feature space with the features extracted from torque, voltage, and current signals in the electric drive system. The output of the neural network system is a vector of k+1 dimensions, $F = \{f_0, f_1, \ldots, f_k\}$. For an input feature vector $\bar{X}$, the neural network system generates the output vector, $F(\bar{X}) = \{f_0(\bar{X}), f_1(\bar{X}), \ldots, f_k(\bar{X})\}$. The diagnostic decision can be derived from $F(\bar{X})$ using the following rules. Let $f_k(\bar{X})$ be $= \max\{f_i(\bar{X}) \mid i = 0, 1, \ldots, k\}$.

- Rule 1: if $f_j(\bar{X}) < T$, then there is an unknown faulty condition in the electric drive.
- Rule 2: if $f_k(\bar{X}) = f_0(\bar{X}) > T$, then the electric drive is in normal operating condition.

- Rule 3: if $f_k(\bar{x}) > T$ and $j > 0$, then the electric drive has a faulty condition that is known as the j^{th} type of faulty condition.

T is a threshold that can be set to a value between 0 and 0.5. For example, if a neural network system is trained to detect and isolate the six single-switch open faults, then k=6, where f_0 represents the normal class, and f_1 through f_6 represent the six single switch faults at A, A', B, B', C and C' (see Figure 1) respectively. For an input vector $\bar{x}$, if $f_2(\bar{x}) = \max\{f_i(\bar{x}) \mid i = 0, 1, \ldots, k\}$ and $f_2(\bar{x}) \geq 0.5$, then it can be concluded that the switch A' in this circuit is broken; if $\max\{f_i(\bar{x}) \mid i = 0, 1, \ldots, k\} < 0.5$, then there is a faulty condition in the circuit, but it is not a single switch fault.

Figure 3 illustrates the computational steps involved in the development of such a neural network system. There are two computational stages: neural learning and fault diagnostic.

The input to the neural learning stage is a training data set that contains 16 groups of signals, $\{\bar{s}_0, \bar{s}_1, \ldots, \bar{s}_{16}\}$, with each group containing seven signals, i.e. three voltage signals, V_{An}, V_{Bn}, V_{Cn}, three currents I_A, I_B, I_C, acquired at the three phases in the inverter (see Figure 1), and the motor electro-magnetic torque T_e. The groups of signals are generated by the simulation model presented in the previous section, under the following conditions. $\bar{s}_0$ contains the seven signals generated under normal operational condition, $\bar{s}_1$ through $\bar{s}_6$ each contains the seven signals acquired under the respective six single switch permanent open conditions, $\bar{s}_7$ through $\bar{s}_9$ each contains the seven signals generated under the three respective post-short-circuit conditions: A and A' open, B and B' open, C and C' open; $\bar{s}_{10}$ through $\bar{s}_{15}$ are the six groups of signals generated under the six short circuit conditions respectively. These groups of signals are segmented and features are extracted on a segment-by-segment basis. The computational steps of signal segmentation and neural learning are described in a subsection below. The result of the neural learning stage is a multi-class neural network that has the capability of detecting and isolating any one of the faulty classes in the six-switch inverter circuit shown in Figure 1.

At the fault diagnostic stage, the segments of the seven signals at the time interval $[t-\Delta w, t]$, where Δw is referred to as the window size, are sent to the feature extraction function to generate a feature vector $\bar{x}$. The description of the feature extraction function is presented in subsection 3.1. The multi-class neural network "CFDNN" (Circuit Fault Diagnostic Neural Network) takes the feature vector $\bar{x}$ as input, and predicts whether there exists a fault in the circuit at time t. If there is a fault, CFDNN points out the type and the location of the fault.

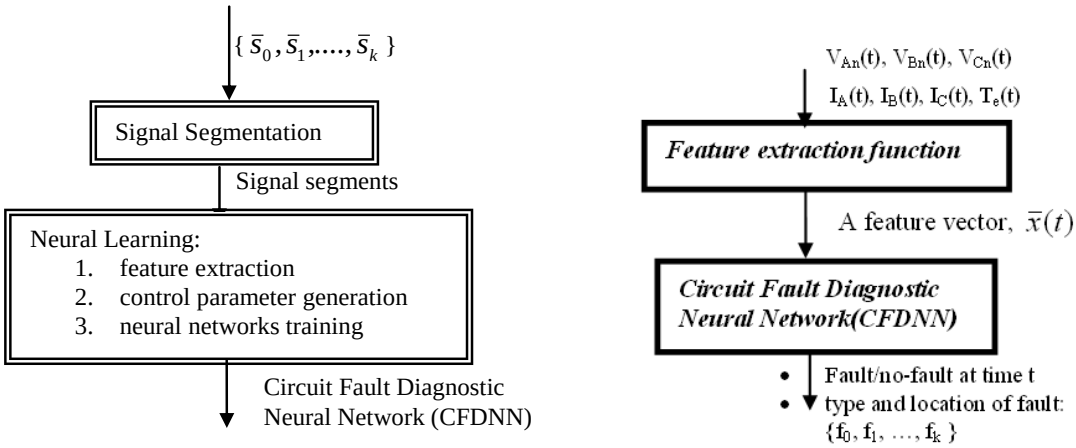

(a). Neural learning of diagnostic knowledge (b) Fault diagnostic stage

Figure 3. A multi-class neural network for circuit fault diagnosis.

3.1 Signal Segmentation and Feature Extraction

In the proposed neural network framework, fault detection and classification is performed by analyzing the signals on a segment-by-segment basis. The basic frequency of the signals generated by the simulation models is about 80 Hz, the sampling frequency is chosen to be 1000 Hz, and the length of a segment is 16 samples. All input signals are segmented using the same fixed window size and the two adjacent segments are overlapped with 5 samples in order to achieve smooth transitions between adjacent windows. For a signal with 3000 data points, it is segmented into 272 segments. Note that all seven signals acquired under the same condition are subject to the same segmentation process.

The following statistical features are extracted from each segment:

- Max: maximum magnitude of the signal within the present segment.
- Min: minimum magnitude of the signal within the segment.
- Median: median of the signal within the segment.
- Mean: mean of the signal within the segment.
- Standard deviation: standard deviation of the signal segment.
- Zero-frequency (i.e. dc) component of the power spectrum.

Since there are seven input signals (three voltage signals, three current signals, and one torque signal), the output from the signal segmentation and feature extraction is a sequence of 42-dimensional (six features are extracted from each of the seven signal segments) feature vectors. The detection of signal faults within a time period is based on the feature vector extracted from the seven signal segments within the current time period by a multi-class neural network.

3.2 A Multi-Class Fault Detection and Isolation Neural Network Framework

A multi-class neural network system maps the input feature space to an output space of more than two classes. Multi-class neural learning involves finding appropriate neural network architecture, encoding schemes, learning algorithms, and training methodology [30]. While binary classification is well understood, multi-class classification has been relatively less investigated. Many pattern classification systems were developed for binary classification problems, but the extension to the multi-class pattern classification is non-trivial, and often leads to unexpected complexity or weak performances [30-32]. The authors developed the following single neural network framework for detecting multi-class signal faults.

One important issue in a multi-class neural network classifier is to design an encoding scheme used to represent the multiple classes in the output nodes of the neural network. The authors chose to use the "one-hotspot" method described as follows. For a k-class classification problem, the neural network system uses a k-bit output layer, i.e. k output nodes. Each class is assigned a unique binary string (codeword) of length k. For example, if the neural network is trained to solve the problem of the six-class single switch fault detection, the output layer should have seven nodes, one representing the normal condition, and the other six nodes representing the six faulty conditions. During the training stage, if a feature vector is extracted from segments of signals representing the normal condition, its target value for the output layer is 1000000, which means only the first output node should produce a value "1", and all other output nodes should output "0". If a feature vector is extracted from the segments representing the switch B faulty condition, its target value for the output layer is 0001000, which means only the 4th output node should produce one value "1" and all others output "0".

In general the multi-class neural network, "Circuit Fault Diagnostic Neural Network" (CFDNN), has one output node to represent the normal condition, and other k output nodes to represent the k classes of faulty conditions. The back propagation algorithm is used to train the neural network. As shown in Figure 3(a), a CFDNN is trained on feature vectors extracted from segments of various signals generated by the simulation program under the normal and various abnormal conditions. At the diagnostic stage, the seven signals, $V_{An}(t)$, $V_{Bn}(t)$, $V_{cn}(t)$, $I_A(t)$, $I_B(t)$, $I_c(t)$, and $T_e(t)$, which can be acquired by the sensors in the circuit, are processed as follows. At time t, the segments of all the seven signals within the window of $(t-\Delta w, t]$ are sent to the feature extraction function (see Figure 3(b)), which generates a feature vector $\bar{x}(t)$ of 42 dimensions from segments $(V_{An}(t-\Delta w), V_{An}(t)]$, $(V_{Bn}(t-\Delta w), V_{Bn}(t)]$, $(V_{cn}(t-\Delta w), V_{Cn}(t)]$, $(I_A(t-\Delta w), I_A(t)]$, $(I_B(t-\Delta w), I_B(t)]$, $(I_C(t-\Delta w), I_c(t)]$, $(T_e(t-\Delta w), T_e(t)]$. For any given feature vector at time t, $\bar{x}(t)$, CFDNN will fire one of its output nodes to indicate whether the circuit at time t is normal or has one of the faulty conditions. If the winning output node has a low value, this indicates that the circuit has an unknown fault. In this paper the authors use the neural network framework to train a system of three neural networks for

diagnostics of the three categories of most critical and frequent circuit faults in a three-phase electric drive model: single switch faults, post-short and short circuit faults.

3.3 CFDNN's for Fault Detection of Open-Switch, Post-Short-Circuit, and Short Circuit

Three CFDNN's were trained to detect and isolate the faulty conditions under any operating state in the speed-torque domain of the electric drive system. All three CFDNN's have the same framework described in section 3.2 above and were trained on the simulation data generated by the inverter based electric drive model described in section 2. In this model, there are two operating parameters, torque and speed, that determine the operating state of the electric drive. Each state dictates the voltage and current signals generated in the drive [20-21]. The entire data for training and test were generated by the operating points shown in the Figure 4. Each operating point, (torque, speed), represents a state in the drive illustrated in Figure 1. These operating points were chosen by a machine learning algorithm "CP-Select", presented in the authors' previous work [20]. At each operating point, the authors ran several simulations using the SIM_drive described in section 2. During each simulation, a normal condition is first simulated for about 0.25 seconds and then a faulty condition is triggered and the simulation continues for about 6 seconds. In each simulation, seven signals, $V_{An}(t)$, $V_{Bn}(t)$, $V_{Cn}(t)$, $I_A(t)$, $I_B(t)$, $I_C(t)$, $T_e(t)$, t= 0, ~ 6.25 sec are extracted and each signal consists of 6000 samples. The data generated by the operating points shown in diamond symbols in Figure 4 were used for training neural networks, and the data generated by the operating points shown in square symbols are for testing.

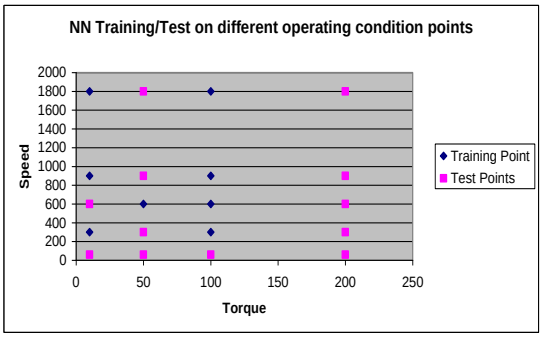

Figure 4. Operating points used for generating, training and testing data.
Torque is measured in the unit of nm, and speed is in rpm.

In order to train a robust neural network, a number of parameters must be carefully chosen including the number of hidden nodes and learning rate [33]. The authors used a three-fold cross validation approach to select the number of hidden nodes and proper learning rate for each type of neural networks. In each fold, 2/3 of the training data were used to train the neural networks and the remaining 1/3 were used as the validation data, the learning rate varied among 0.005, 0.01, 0.05 and 0.1, and

the number of hidden nodes varied among 10, 15, 20, and 25. In each run, the stop criterion is a combination of the maximum epoch number and the threshold of error: if the number of the epoch has reached 5000 or the minimum squared error is less than 1E-3, then the training stops. The learning rate did not seem to have much impact on the performances on the validation data for all neural networks. Therefore the authors chose to use 0.01 in the final training of the neural networks. The authors evaluated the performances of each type of neural networks averaged over three validation set and found that the three neural networks with 20 hidden nodes gave the most robust performances. Based on the above analysis, the following three neural networks were trained.

The CFDNN trained for detecting the single switch faults has 42 input nodes representing the 42 dimensions of the feature vector, seven output nodes representing the normal condition and the six single switch faults (for switches A, A', B, B', C, C'), and one hidden layer with 20 nodes. The CFDNN trained for detecting the post-short-circuit faults has 42 input nodes, one hidden layer with 20 nodes, and four output nodes representing the normal class and the three faulted classes of the post-short-circuit. The simulation data for the three post-short-circuit faults were generated by making one vertical switch pair open at a time, namely, the pairs A and A', B and B', and C and C' (see Figure 1). The CFDNN trained for detecting the short circuit faults in the six-switch inverter scheme has 42 input nodes, one hidden layer with 20 nodes, and seven output nodes representing the normal class and the six faulty classes of short circuits: A short, A' short, B short, B' short, C short and C' short.

The performances of all three neural networks on the test data generated by SIM_drive using the 12 test points shown in squares in Figure 4 are presented in Figure 5 (a). In order to test the robustness of the system against noise, the authors added 3% of noise to all the data generated by SIM_drive. The performances of the three neural networks trained on the noise data are shown in Figure 5 (b). Let the 12 test points be $\{(s_i, t_i) \mid i = 1, \ldots, 12\}$. $\Phi_{n,c}((s_i, t_i))$ is the correct detection rate of the c^{th} class of faulty conditions by the n^{th} neural network when the circuit is operating at the point (s_i, t_i), where n =1 is the neural network trained to detect the six classes (c = 1, …, 6) of single switch open, n=2 is the neural network trained to detect the three classes of post-short circuit faults (c = 1, 2, 3), and n = 3 is the neural network trained to detect the six classes (c = 1, …, 6) of short circuit faults. The blue bars in Figure 5 depict the average detection rate made by the neural network trained to detect the single switch open faults:

$$\overline{\Phi}_{1,c} = \frac{1}{12}\sum_{i=1}^{12}\Phi_{1,c}(s_i, t_i) \tag{2}$$

where c = 0 represents the normal class, and c = 1, …, 6 represent F1 … F6 that correspond to the faulty classes of A, A', B, B' and C and C' open respectively. On the noise-free test data (see Figure 5 (a)), more than 97.5% of all the normal signal

segments were detected correctly; two classes of faults, the B' (F4) and C (F5) open faults, are detected correctly in 100%; over all the classes, the normal and the six faulty classes, more than 99% (shown in the "overall" category) of signal segments are detected correctly. On the test data with added noise, the performances (see Figure 5 (b)) of all classes dropped in comparison to the noise-free data except for classes F1 and F6. The overall detection rate on noise data is around 97.5%.

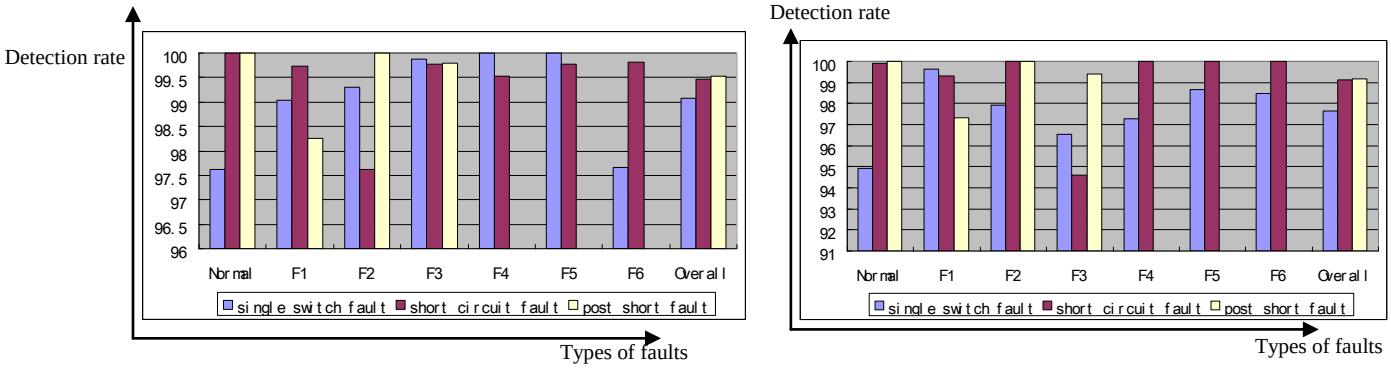

(a) Performance without noise.

(b) Performance with noise present.

Figure 5. System performances of 15 classes of faults on test data without or with noise. Blue bars mark the accuracy of detecting single open switch faults, yellow bars mark the accuracy of detecting post-short faults, and the burgundy bars mark the accuracy of detecting short circuit faults.

The yellow bars in both Figure 5(a) and (b) depict the performance of the post-short fault detection neural network calculated using the following formula:

$$\overline{\Phi}_{2,c} = \frac{1}{12}\sum_{i=1}^{12}\Phi_{2,c}(s_i, t_i) \tag{3}$$

for c = 0, 1, 2, 3. The post short circuits have only three classes of faults, A and A' open represented by c = 1 or F1, B and B' open represented by c = 2 or F2, and C and C' open represented by c = 3 or F3. Note that F4 through F6 are not applicable for this neural network. On the noise free test data (see Figure 5(a)), the detection rates for the normal class and the F2 fault, i.e. B and B' both are open permanently, are 100% in accuracy. The average detection accuracy over all classes reached 99.5%. On the noisy data (see Figure 5(b)), the performance drops slightly in each class, and the overall detection rate is 99%.

The burgundy bars in both Figure 5(a) and (b) depict the performances of the neural network trained to detect the short circuit faults. The performances are calculated using the following formula:

$$\overline{\Phi}_{3,c} = \frac{1}{12}\sum_{i=1}^{12}\Phi_{3,c}(s_i, t_i) \tag{4}$$

for c = 0, … 6 where c = 0 represents the normal condition, c = 1 or F1 through c = 6 or F6 represent respectively the short circuit classes of single switches, A, A', B, B', C and C' closed. On the noise free test data, the system detected more than 99.5% of the faults correctly over all classes except for the F2 class, i.e., the A' short class, which is detected correctly at a rate

of 97.5%. On the noise test data, the overall performance is at 99%, which is only slightly down from 99.5% on the noise free data.

To further study the noise effects, the authors randomly selected three test points, OP1 = (10, 600), OP2 = (50, 900), and OP3 = (200, 60), and then added three levels of noise: 5%, 10%, and 15%, to the test data generated from these points. The system performances are illustrated in Figure 6. At each operating point (OP), the average fault detection accuracies over all 15 classes of faults are shown on the data without noise (in blue bars), data with 5% noise (in burgundy bars), 10% noise (in very light yellow bars), and 15% noise (in aquamarine bars). For the data generated at OP1, the performance dropped from 99.8% to 99.3% on the data with 5% and 10% added noise, and dropped to 98.4% on the data with 15% added noise. For the data generated by OP2 and OP3, the performances stayed at 100% detection accuracy on the data generated with 0%, 5% and 10% added noise. The performances dropped slightly (to 98.8% on OP2 data and to 99.4% on OP3 data) when 15% noise were added to the data. Over all the operating points, the noise data has very little effect on the system performances.

Based on the above comparative study of the system performances on the noise free data and the data with different levels of noise, it can be concluded that the proposed three CFDNN systems are robust to data noise.

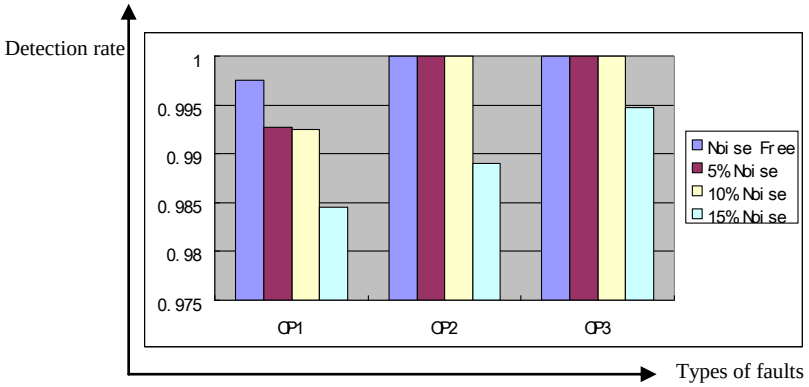

Figure 6. Analysis of noise effects on neural network performances on test data generated by three operating points, OP1, OP2, and OP3.

4 REAL-TIME ELECTRICAL DRIVE FAULT DETECTION AND CLASSIFICATION

The most challenging aspect in an electric circuit diagnostic system is to detect a fault immediately after it occurs and pin-point to the cause of the faults. As soon as a fault is detected and isolated where it is, e.g. A short or C' open etc., it is possible to either isolate or shut down the faulty part of the circuit to minimize the damage. The knowledge about the type of fault, e.g. switches A and A' are open, can lead to fast recovery from failure. In this section the authors present a structured diagnostic neural network system that is designed to detect, in real time, any of the 15 faults, i.e. 6 single switch open faults, 3 post-short circuit faults, and 6 short circuit faults, described in the last section. Figure 7(a) shows the schematic drawing of the system.

The three neural networks NN1, NN2 and NN3, discussed in the last section are employed in the real-time fault detection and classification system, where NN1 is trained to detect any of the six single switch open faults, NN2 is the neural network trained to detect any of the three post-short-circuit faults, and NN3 is the neural network trained to detect any of the six short circuit faults. The decision logic is described as follows. Let the j^{th} output function of the i^{th} neural network be f_i^j, where j = 0, …, 6 when i = 1 or 3, and j = 0, …3, when i = 2. Let the feature vector at time t be $\bar{x}(t)$. The decision function involves the following steps of calculation.

First it finds the neural network, i, that has the highest confidence at its c^{th} output node among all output nodes of all three neural networks:

$$f_i^c = \max_{j=0,\ldots,6,k=0,\ldots,3,m=0,\ldots,6} \{ f_1^j(\bar{x}(t)), \; f_2^k(\bar{x}(t)), f_3^m(\bar{x}(t)) \tag{5}$$

If f_i^c < T, a threshold such as 0.5, then the circuit has an unknown fault, i.e. the fault is not any of the single open switch faults, or any of the post-short-circuit faults, or any of the six short circuit faults. Otherwise, if c = 0, then the entire circuit is normal, and if c > 0 then the circuit has one of the 15 faults. The type and location of the fault is identified through the following calculation. If (i =1) and (c > 0), it is one of single switch open faults and the location of the fault is indicated by c, which indicates which one of the six switches is the faulty one. If (i = 2) and (c > 0), the type of the fault is post-short, and c indicates which branch of the circuit has the post-short fault. For example c = 1 indicates that the branch A and A' has the post-short fault. If (i = 3) and (c > 0), the type of the fault is short circuit, and c indicates which of the six switch is shorted.

For the purpose of comparison, the authors also implemented a single neural network to classify all 16 classes: normal, 6 single switch open faults, 3 post-short-circuit faults, and 6 short circuit faults. The schematic drawing of this neural network system is shown in Figure 7 (b). The neural network has the same input layer as all the three neural networks in the structured system in Figure 7(a), however it has an output layer of 16 nodes, one represents the normal class, and the other 15 represent the 6 single switch open faults, 3 post-short faults and 6 short circuit faults. All neural network systems were trained and tested on the same data generated at the operating points illustrated in Figure 4. The objective of the two systems is to detect and identify any of the 15 faults as soon as they occur. Therefore the performance of such a system is measured by the time needed to detect and isolate any of the 15 faults after its occurrence.

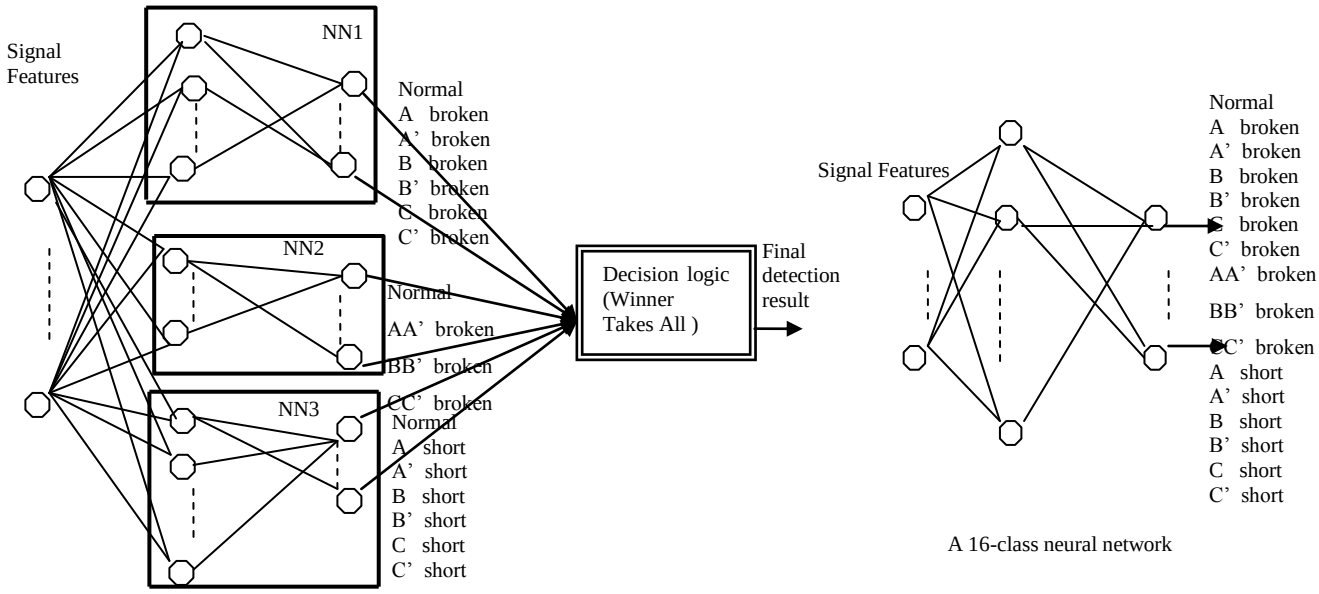

(a). A structured neural network system

(b). A single multi-class neural network system

Figure 7: Two architectures of neural network systems for classifying multiple classes of faults in a three-phase electric drive.

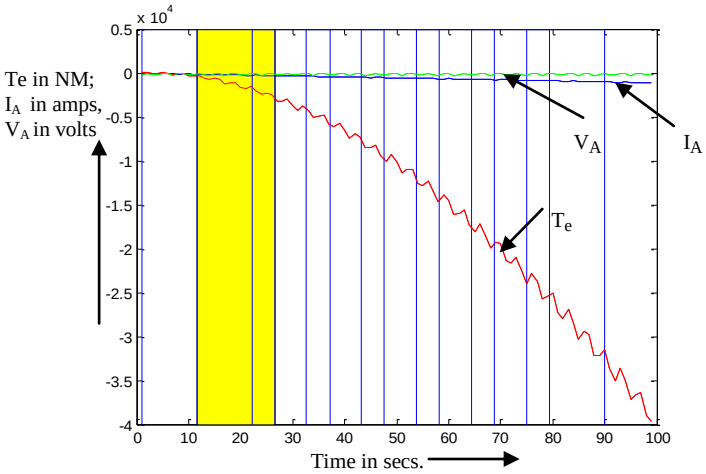

Figure 8. The Switch A open case under T_e=200 Sp=900 operating condition. The shaded segment is the first segment being detected by the CFDNN after switch A is broken. Horizontal axis is time in msec.

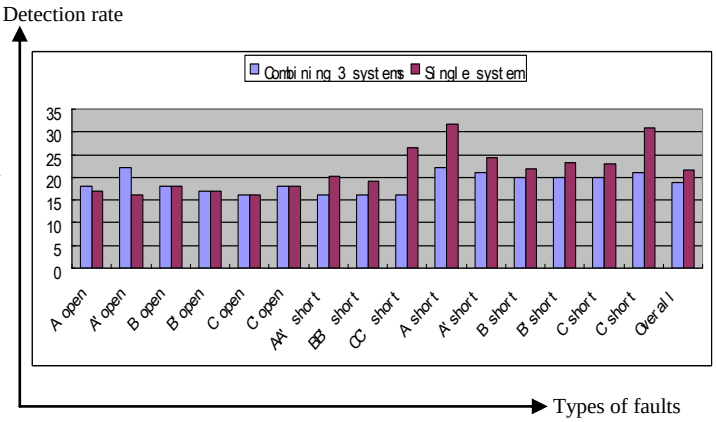

Figure 9. Performances of the two neural network systems

Let t_0 be the time at which a fault occurs. If a faulty condition is first detected at time t based on features extracted from the segments of the signals between the time interval $[t-\Delta w, t]$, the time that the system takes to detect this faulty condition is $t_d = (t - t_0)$. Figure 8 illustrates this concept. In the figure three signals are displayed, the current and voltage measured at switch A, and the torque signal under the operation condition with switch A broken. The shaded segment is the first segment that is detected correctly by the structured neural network system. In this implementation, Δw = 16 ms, and every two adjacent

segments are overlapped by about 5 ms. In this example, the faulty segment was detected at t = 27 ms, the faulty condition occurred at time t_0 = 11 ms, therefore, t_d = 16 ms, which implies that the faulty condition was detected within 16 ms.

Figure 9 illustrates the performances of the two neural network systems on the test data generated by 12 operating points shown in Figure 4. The performance of a fault detection system is evaluated by the amount of time it takes to detect and isolate the faulty condition correctly after a fault occurs. The horizontal axis in Figure 9 indicates the 15 faulty classes and the average over all 15 classes, and the vertical axis indicates the time in milliseconds, which the two systems took to detect correctly each of the faulty classes.

The blue bars show the performance of the proposed structured neural network system, and the burgundy bars show the performance of the single neural network system. Except for A and A' open, the proposed structured neural network system correctly detects and identifies all the faulty classes in less time than the single neural network system. Most of the faulty classes were correctly detected by the structured neural network system in less than 20 ms. This implies that the faulty conditions were detected as soon as they occurred. Only two classes of faults were correctly detected at 23 ms after the faults occurred, which implies that the system detected the faults correctly at the second segment after the faulty conditions occurred.

5 SUMMARY AND CONCLUSIONS

The authors have presented an intelligent system based diagnostic approach for the detection and isolation of a broad range of faults in electric drive inverters in closed-loop systems. A model of the electric drive inverter with a three-phase induction motor and a control mechanism was developed that successfully simulates the normal operations of the power electronics inverter, six single switch open fault conditions, three post-short-circuit conditions, and six short circuit conditions under closed-loop field oriented control. This model has been implemented using a generic commercial simulation tool [22] to generate signals for neural learning of diagnostic features. Three important sets of signals, namely the torque, and voltages and currents in different phases were used for the fault diagnostics. These signals were segmented simultaneously and diagnostic features were extracted from signal segments. A multiple class neural network framework, CFDNN, has been presented. Three neural networks were developed under the framework for the detection and isolation of single switch open faults, post-short circuit faults, and short circuit faults. The accuracy of the diagnostic results has reached more than 99% in average. Furthermore, the authors presented a structured neural network system that is trained to detect and isolate any of the 15 faults in a three-phase induction motor in real-time. The system performance is evaluated on the basis of time elapsed to detect a fault after it occurs. The simulation results show that the proposed system takes less than 20 ms on an average to successfully detect and isolate a fault.

In conclusion it can be said that the proposed model-based fault diagnostic approach combined with machine learning techniques is effective in reliably detecting and isolating faults occurring in power electronics inverter based electric drives in real-time.

6 ACKNOWLEDGMENTS

The research described in this paper was supported through a funding by the US Army RDECOM-TARDEC ILIR (In-house Lab. Independent Research) program.

7 REFERENCES

[1] Chan, C., and Chau, K.: 'Modern electric vehicle technology', (Oxford University Press, 2001).
[2] Novotny, D., and Lipo, T.: 'Vector control and dynamics of AC drives', (Oxford Sc. Pub., 1996).
[3] Kao, N., and Liu, C.: 'Analysis and design of microprocessor-based vector-controlled induction motor drives', IEEE Trans. on Ind. Electronics, Vol 39., No. 1, Feb. 1992, pp. 46-54.
[4] Masrur, M., Xu, X., and Liang, F.: 'Fault Isolation in an Induction Motor Control System', U.S. Patent 5469351, Nov 1995.
[5] Klima, J.: 'Analytical investigation of an induction motor drive under inverter fault mode operations', IEE Proc.- Electr. Power Appl., Vol 150, No. 3, May 2003, pp. 255-262.
[6] Gertler, J., Costin, M., Fang, X., Kowalczuk, Z., Kunwer, M., Monajemy, R.: 'Model Based Diagnosis for Automotive Engines-Algorithm Development and Testing on a production Vehicle', IEEE Trans on Control Systems Technology, Vol. 3, No. 1, 1995.
[7] Nyberg, M.: 'Model-based Diagnosis of an Automotive Engine Using Several Types of Fault Models', IEEE Transaction on Control Systems Technology, Vol. 10, No. 5, pp 679-689, 2002.
[8] Ribeiro, R., Jacobina, C., Silva, E.: 'Fault Detection of Open-Switch Damage in Voltage-Fed PWM Motor Drive System', IEEE Trans on Power Electronics, Vol. 18, No. 2, March 2003, pp 587-593.
[9] Zidani., F., Benbouzid, M., Diallo, D., and Said, M.: 'Induction Motor Stator Faults Diagnosis by a Current Concordia Pattern-Based Fuzzy Decision System', IEEE Trans. on Energy Conversion, Vol. 18, No. 4, Dec 2000, pp. 469-475.
[10] Benbouzid, M.:'Bibliography on Induction Motor Faults Detection and Diagnosis', IEEE Trans. on Energy Conversion, Vol. 14, No. 4, Dec 1999, pp. 1065-1074.
[11] Nelson, A., and Chow, M.: 'Characterization of coil faults in an axial flux variable reluctance PM motor,' IEEE Trans. on Energy Conversion, vol. 17, pp. 340-348, 2002.
[12] Ayhan, B., Chow, M., and Song, M.: 'Multiple Signature Processing-Based Fault Detection Schemes for Broken Rotor Bar in Induction Motors', IEEE Trans. on Energy Conversion, Vol. 20, No. 2, June 2005, pp. 336-343.
[13] B. Lu and S. Sharma, "A literature review of IGBT fault diagnostic and protection methods for power inverters," in Proc. the 43rd IEEE Industrial Applications Society Annual Meeting (IAS'08), Oct. 2008.
[14] Fenton, F., McGinnity, T., and Maguire, L.: 'Fault diagnosis of electronic systems using intelligent techniques: a review', IEEE Trans. on Systems, Man, and Cybernetics – Pt. C, Vol. 31, No. 3, Aug 2000, pp. 269-281.
[15] Feldkamp, L., and Puskorius, G.: 'A Signal Processing Framework Based on Dynamic Neural Networks with Application to Problems in Adaptation, Filtering, and Classification,' Proceedings of The IEEE, Vol. 86, No. 11, November, 1998.
[16] Murphey, Y., Guo, H., Crossman, J., and Coleman, M.: 'Automotive Signal Diagnostics Using Wavelets and Machine Learning,' IEEE Transaction on Vehicular, November, 2000.
[17] Crossman, J., Guo, H., Murphey, Y., and Cardillo, J.: 'Automotive Signal Fault Diagnostics: Part I: signal fault analysis, feature extraction, and quasi optimal signal selection,' IEEE Transaction on Vehicular, July 2003
[18] Murphey, Y., Crossman, J., Chen, Z., and Cardillo, J.: 'Automotive Fault Diagnosis Part II A Distributed Agent Diagnostic System,' IEEE Transaction on Vehicular, July 2003.
[19] Chen, Z., Murphey, Y., Zhang, B., Jia, H., Masrur, M.: 'Robust Fault Diagnosis in Electric Drives Using Machine Learning', IEEE VPPC 2004
[20] Murphey, Y L, Masrur, M A, Chen, Z H, Zhang, B.: 'Model-Based Fault Diagnosis in Electric Drives Using Machine Learning', IEEE Trans. On Mechatronics, vol. 11, No. 3, June, 2006, pp. 290-303.
[21] Masrur, M., Chen, Z., Murphey, Y.: 'Model-Based Fault Diagnosis in Electric Drive Inverters Using Artificial Neural Networks', IEEE-PES Annual Meeting , Panel Session Tampa, June 24-28, 2007, CD-ROM
[22] Mathworks, 'Matlab-Simulink Reference Manual'.
[23] Masrur, M A.: 'Assumption or Fact ? - Line-to-Neutral Voltage Expression in an Unbalanced 3-Phase Circuit During Inverter Switching,' IEEE Transaction on Education, Accepted for publication, 2008.
[24] Bishop, C..: 'Neural Networks for Pattern Recognition' (Oxford University Press, 1995).
[25] LeCun, Y., Bottou, L., Bengio, Y., and Haffner, P.: 'Gradient-Based Learning Applied to Document Recognition,' Proceedings of the IEEE, (86) 11, pp. 2278-2324, 1998.
[26] Huang, W., and Lippmann, R..: 'Neural net and traditional classifiers'. in D. Z. Anderson (Ed.), Neural Information Processing Systems, pp. 387-396. New York: American Institute of Physics.
[27] Allwein, E., Schapire, R.: 'Reducing Multiclass to Binary: A Unifying Approach for Margin Classifiers,' Journal of Machine Learning Research 1, pp. 113-141, 2000.
[28] Har-Peled, R., and Zimak, D.: 'Constraint classification: A new approach to multiclass classification', in Proc. 13th International Conf. of Algorithmic Learning Theory, pages 365–397, 2002.

[29] Ou, G., Murphey, Y., Feldkamp, L.: 'Multiclass Pattern Classification Using Neural Networks', Int. Conf. On Pattern Recognition, Cambridge, UK, 2004.
[30] Anand, R., and Mehrotra, K.: 'Efficient Classification for Multiclass Problems Using Modular Neural Networks', IEEE Trans. On Neural Networks, vol. 6, no. 1, Jan 1995, pp. 117-124.
[31] Gelenbe E., and Hussain, K.: 'Learning in the Multiple Class Random Neural Network', IEEE Trans. On Neural Networks, vol. 13, no. 6, Nov. 2002, pp. 1257-1267.
[32] Ou, G., and Murphey, Y.: 'Multi-class Pattern Classification Using Neural Networks,' Journal of Pattern Recognition, Vol. 40, Issue 1, January 2007, Pages 4-18.
[33] Hastie, T., Tibshirani, R., and Friedman, J.: 'The Elements of Statistical Learning: Data Mining, Inference, and Prediction', 2nd. Edition, (Springer, 2009).